DOE/SERI-8119-3/2-T6
Distribution Category UC-63

SEQUENTIAL PURIFICATION AND CRYSTAL GROWTH FOR THE PRODUCTION OF LOW COST SILICON SUBSTRATES

Quarterly Technical Progress Report No. 3, April 1—June 30, 1980

By
Ming Liaw
Frank Secco D'Aragona

August 1980

Work Performed Under Contract No. AC02-77CH00178

Motorola, Inc.
Semiconductor Group
Phoenix, Arizona

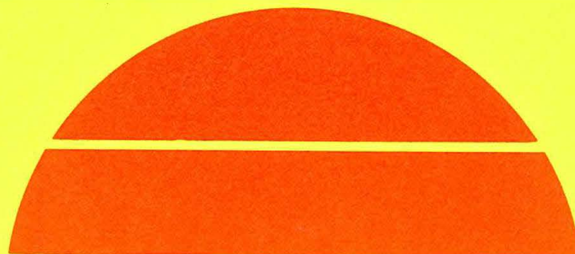

U.S. Department of Energy

Solar Energy

DISCLAIMER

"This book was prepared as an account of work sponsored by an agency of the United States Government. Neither the United States Government nor any agency thereof, nor any of their employees, makes any warranty, express or implied, or assumes any legal liability or responsibility for the accuracy, completeness, or usefulness of any information, apparatus, product, or process disclosed, or represents that its use would not infringe privately owned rights. Reference herein to any specific commercial product, process, or service by trade name, trademark, manufacturer, or otherwise, does not necessarily constitute or imply its endorsement, recommendation, or favoring by the United States Government or any agency thereof. The views and opinions of authors expressed herein do not necessarily state or reflect those of the United States Government or any agency thereof."

This report has been reproduced directly from the best available copy.

Available from the National Technical Information Service, U. S. Department of Commerce, Springfield, Virginia 22161.

Price: Paper Copy $6.00
Microfiche $3.50

TABLE OF CONTENTS

		Page
I.	INTRODUCTION	1
II.	THEORETICAL CONSIDERATION	1
	1. Purification by Vacuum Treatment	1
	2. Purification by Impurity Redistribution	5
III.	EXPERIMENTALS	8
	1. Vacuum Treatment in a Multiple Zone Furnace	8
	2. Vacuum Treatment in a Crystal Puller	10
	2.1 Results and Discussion	11
	3. Purification by Impurity Redistribution	14
	3.1 Results and Discussion	14
	3.1.1 Impurity Concentration as Function of Distance from the Seed	14
	3.1.2 Large Grain vs. Growth Rate	17
	3.1.3 Impurity Concentration vs. Grain Size	22
IV.	CONCLUSION AND RECOMMENDATIONS	26
V.	PLANS FOR THE NEXT QUARTER	26

LIST OF TABLES

		Page
Table I	Boiling point (^{o}C) of the impurities of concern in MG-Si as function of two vapor pressures.	2
Table II	Estimated values of $\overline{\Delta H}$, ΔG^{o} and E^{-1} for some impurities at the melting point of silicon.	4
Table III	Segregation coefficients for various metallic impurities for different crystal growth conditions.	6
Table IV	Comparison of impurity concentration in MG-Si ingots purified by: (A) vacuum treatment of slag, (B) physical separation of slag.	13
Table V	Variation of impurity concentration along the length of a MG-Si ingot. (ppmw)	19
Table VI	Comparison of impurity concentration as function of grain size at the seed and tang ends of two MG-Si ingots. Analysis by emission spectroscopy. (ppmw)	23
Table VII	Comparison of impurity concentration as function of grain size at the seed and tang ends of two MG-Si ingots. Analysis by spark source mass spectroscopy. (ppmw)	24
Table VIII	Comparison of impurity concentration at the seed and tang ends of two large-grained MG-Si ingots with two SG crystals. Analysis by spark source mass spectroscopy. (ppmw)	25

LIST OF FIGURES

		Page
Figure 1.	(A) Apparatus used for vacuum evaporation experiments, (B) temperature profile of the deposition zone and elements deposited on the various zones.	9
Figure 2.	Disappearance of slag from MG-Si melt by vacuum treatment. (A) slag on MG-Si melt, (B) melt boiling, (C) melt free of slag.	12
Figure 3.	Three inches (100) shoulder used to initiate ingot growth.	15
Figure 4.	Polycrystalline growth induced by poor blending of a large seed with the silicon melt.	16
Figure 5.	MG-Si ingot grown using a 3" (100) shoulder as a seed and relative cross sections.	18
Figure 6.	Comparison of grain size as a function of growth rate and distance from the seed.	20
Figure 7.	Comparison of grain size as a function of seed size and growth rate at the seed and tang ends of three MG-Si ingots.	21

I. INTRODUCTION

The objective of this program is to identify and develop low cost processing for fabricating large grain size polycrystalline silicon substrates. Metallurgical grade silicon (MG-Si) is chosen as the starting material for sequential purification and crystal growth. As shown in the previous two technical reports,[1,2] several purification techniques have been studied. They include (1) acid leaching with HCl, (2) physical separation of insoluble impurities, (3) reactive gas treatment of molten silicon, and (4) slagging using a mixed-oxide slag. In this quarterly period purification by vacuum treatment and by impurity redistribution using ingot pulling has been studied.

II. THEORETICAL CONSIDERATION

1. Purification by Vacuum Treatment

The purpose of applying a vacuum to a crystal puller which contains a MG-Si charge is to enhance evaporation of impurities in silicon. Evaporation may occur in two stages. The first is during the heating of the MG-Si charge prior to melting. The second is the evaporation from the molten solution after the silicon charge has melted. The rate of evaporation of elemental impurities from a solid charge is primarily determined by the vapor pressure of the impurity. Table I lists the relationship between the vapor pressure and temperature of impurities contained in MG-Si. Column 3 of Table I shows that at one atmosphere Cl, P, K, As, Cd, Na and Mg boil at a temperature below the melting point of silicon (1412°C). When a vacuum is applied and the pressure is reduced to 10^{-4} atmosphere, the boiling point of the impurities is decreased as shown in column 2. It also shows that at this pressure the additional impurities, Ca, Sb, In, Mn, Ga, and Al boil at a temperature below the melting point of Si. Thus the purification of MG-Si can be improved by applying a vacuum to a heated MG-Si charge.

TABLE I

BOILING POINT (^{o}C) OF THE IMPURITIES OF CONCERN IN MG-Si AS FUNCTION OF TWO VAPOR PRESSURES

	10^{-4} ATm	1 ATm
Cl	-134	-34
P	23	280
K	261	779
As	290	622
Cd	312	765
Na	350	914
Mg	516	1126
Ca	688	1482
Sb	752	1617
In	1077	2167
Mn	1087	2097
Ga	1227	2427
Al	1272	2327
Cu	1412	2595
Si*	1467	2477
B	1477	2527
Fe	1564	2735
Ni	1657	2837
Ti	1717	3127
Co	1827	3097
V	2067	3527
Zr	2177	3577
Mo	2727	4804
C	2897	4502

Table I also lists the impurities of low vapor pressure, which can hardly be removed by evaporation. These elements are the transition metals, Mo, Zr, B and C. Fortunately these impurities (with the exception of B) have a very low segregation coefficient and can be easily removed by an ingot pulling technique as described in Section II-2.

Evaporation of impurities from molten silicon is not simply related to their vapor pressure. Other thermodynamic constants are needed to predict the volatility of the solute from a molten solution. For a dilute liquid solution of an impurity in silicon, the variation of impurity concentration, due to evaporation in a vacuum can be expressed as[3]

$$\frac{dC\ell}{dt} = -\frac{AEC\ell}{W\ell} \qquad (1)$$

where:
- A = area of evaporation surface
- $C\ell$ = concentration of impurities
- $W\ell$ = weight of molten silicon

with:

$$E = \frac{\beta\, Ms}{\sqrt{2\pi MRT}} \exp \frac{(\overline{\Delta H}-\Delta G^o)}{RT} \qquad (2)$$

where:
- β = constant
- Ms = molecular weight of silicon
- M = molecular weight of impurity
- $\overline{\Delta H}$ = partial molal heat of solution
- ΔG^o = molal free energy of evaporation
- R = gas constant
- T = absolute temperature

Equations (1) and (2) show that the evaporation rate is primarily determined by the difference between the partial molal heat of solution and molal free energy of evaporation ($\overline{\Delta H}-\Delta G^o$). The values of $\overline{\Delta H}$ and ΔG^o for some impurities in molten silicon are listed in Table II. The smaller the negative value of ($\overline{\Delta H}-\Delta G^o$),

TABLE II

ESTIMATED VALUES OF $\overline{\Delta H}$, ΔG^{o} and E^{-1}
FOR SOME IMPURITIES AT THE MELTING POINT OF SILICON (after Ref.3)

ELEMENT	$\overline{\Delta H}(K_{cal})$	$\Delta G^{o}(K_{cal})$	E^{-1}
P	-50	+18	5×10^{3}
As	-34	+16	1×10^{2}
Sb	- 5	- 2	6
In	- 1	- 1	1×10^{2}
Mn	-10	-10	2×10^{3}
Ga	- 1	-21	4×10^{2}
Al	- 4	-28	5×10^{3}
Cu	- 3	-31	1×10^{4}
B	-10	-34	1×10^{5}
Fe	+ 6	-42	2×10^{4}

the smaller the value of E^{-1}. The calculated E^{-1} for these impurities are also given in Table II. The smaller the E^{-1} value the greater the evaporation rate from the molten silicon solution. Note that the sequence of E^{-1} values for various impurities (i.e., $Sb < As < In < Ga < Mn < Al$ etc.) is different from that of the boiling point of impurities ($P < As < Sb < In < Mn$ etc.).

2. Purification by Impurity Redistribution

Purification by impurity redistribution upon ingot pulling perhaps is the most effective method for removing metallic impurities from the MG-Si. Table III lists the segregation coefficients for various metallic impurities in silicon. It can be seen that most of the metallic impurities have a segregation coefficient less than 10^{-3} with the exception of aluminum. In other words upon melting and ingot pulling the metallic impurities in the solidified silicon will be approximately three orders of magnitude purer than that in the remaining melt.

More precisely the impurity concentration in the pulled ingot is related to the impurity concentration in the original melt and the segregation coefficient by the following equation:

$$C_s = K\, C_{o\ell}\, (1-g)^{K-1} \qquad (3)$$

where: C_s is the impurity concentration in the pulled ingot
$C_{o\ell}$ is the impurity concentration in the original melt
K is the segregation coefficient of the impurity.

In the actual crystal pulling the segregation coefficient is varied with the crystal pulling parameters. Therefore the effective segregation coefficient K_{eff} is used. The effective segregation coefficient is related to the equilibrium segregation coefficient K_o and the crystal parameters as follows:

$$K_{eff} = \frac{K_o}{K_o + (1-K_o)\exp(\frac{-V\delta}{D})} \qquad (4)$$

TABLE III

SEGREGATION COEFFICIENTS FOR VARIOUS METALLIC IMPURITIES IN SILICON FOR DIFFERENT CRYSTAL GROWTH CONDITIONS

Impurity Element	Single Crystal	ref.	Polycrystalline	ref.	Constitutionally Super Cooled	ref.
Al	2.8×10^{-3} to 3×10^{-2}					
Ga	8×10^{-3}					
Bi	7×10^{-4}					
Cu	6.9×10^{-4}		1.7×10^{-2}		0.16	
Zn	1×10^{-5}					
Au	2.5×10^{-5}					
Fe	6.4×10^{-6}					
Co	8×10^{-6}					
Te	4×10^{-6}					
Cd	1×10^{-8}					
Mn	1.3×10^{-5}		5.7×10^{-2}		0.429	
Mg	3.2×10^{-6}					
Ni	3.2×10^{-5}					
Ti	3.6×10^{-6}					
V	4×10^{-6}					
Zr	$<1.5 \times 10^{-7}$					
Cr	1.1×10^{-5}					

where: V is the crystal pull rate

δ is the thickness of boundary layer at the solid-liquid interface

D is the diffusion coefficient of the impurity at at the interface.

Equation 4 shows that effective segregation varies with the ingot pull rate. When the ingot pull rate is decreased to zero the effective segregation coefficient approaches the equilibrium segregation coefficient. When the ingot pull rate is increased to infinity, the effective segregation coefficient becomes one. In this case no purification takes place by ingot pulling. Equation 4 also shows that K_{eff} is affected by the thickness of the boundary layer δ. A smaller value of δ is needed for a smaller K_{eff} value. A high rate of crystal and/or crucible rotation will lead to a decrease in δ.

The effective segregation coefficient also varies with the grain size and grain structure of the ingot being pulled. The effective segregation coefficient is greatly increased when the ingot is pulled from a melt of constitutional supercooling or when the pulling ingot contains very small grain size. Table III illustrates the change of segregation coefficient of Cu and Mn under three different crystal pulling conditions. It is therefore important that the constitutional supercooling is prevented. The conditions in which the constitutional supercooling can be prevented is given by:

$$\frac{G}{V} \geqslant \frac{mC_o(0)(1-K_o)}{K_o D} \qquad (5)$$

where: G is the temperature gradient of the melt

V is the crystal pull rate

m is the slope of the binary phase diagram of silicon and impurity of interest

$C_o(0)$ is the impurity concentration in the solid at the solid-liquid interface

K_o is the equilibrium segregation coefficient

D is the impurity diffusion coefficient in the melt.

Thus in order to prevent constitutional supercooling, the term on the left hand side of equation 5 has to be greater than that on the right hand side of the equation. This can be achieved either by the increase in G and/or the decrease in ingot pull rate V.

The ingot formation task carried out in this quarter was aimed to develop the techniques for prevention of constitutional supercooling and the growth of large grain ingots.

III. EXPERIMENTALS

1. Vacuum Treatment in a Multiple Zone Furnace

MG-Si has been heat treated at 1350°C under a vacuum for the evaporation study. These experiments were carried out under Motorola's in-house project[4]. Figure 1,A shows the sketch of the apparatus used for this study. An MG-Si charge was contained in a 4" diameter closed-bottom quartz tube. The extension of the quartz tube was reduced to 2" in diameter and contained a free space. The quartz tube was placed in a multiple zone furnace with a temperature profile shown in Figure 1,B. When the MG-Si charge was heated at a vacuum of 10^{-3} torr, impurities evaporated from the MG-Si and condensed on the inner wall of the upper quartz tube. A few hours of heat treatment resulted with deposition of a continuous layer of film on the 550°C to 1100°C temperature zone.

The film deposited in each temperature zone exhibits a characteristic metallic luster.

Samples of deposited film were taken with a given increment of length along the axis of the quartz tube. The emission spectrographic technique was used to identify the impurities in the deposited film. Figure 1,B lists the impurities. The position of the row listing the impurities is approximately the same as the position shown in Figure 1,A from which the samples were taken. By comparison of the elements listed in Figure 1,B

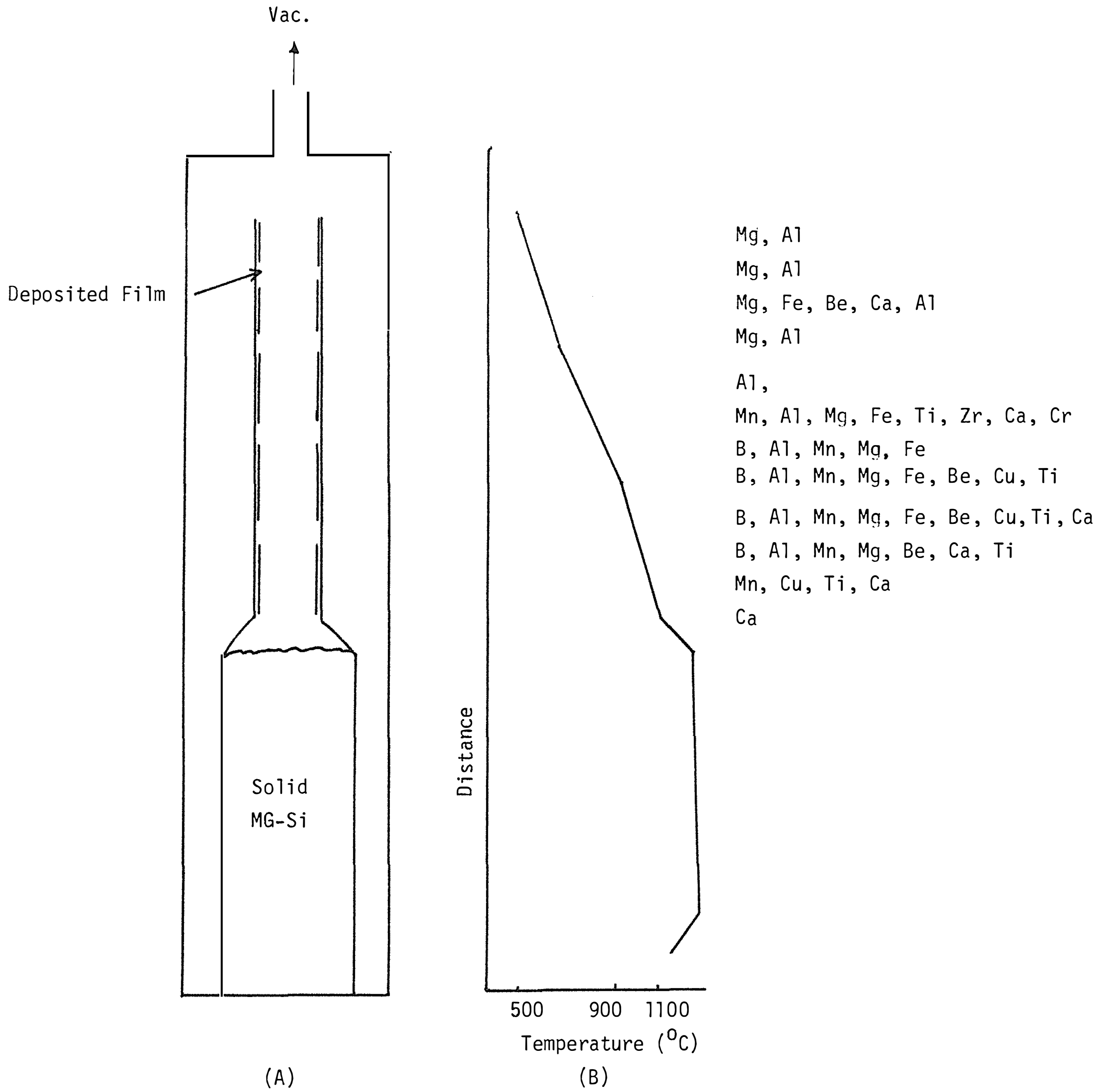

Figure 1. (A) Apparatus used for vacuum evaporation experiments, (B) Temperature profile of the deposition zone and elements deposited on the various zones.

with the boiling point data shown in Table I, it can be seen that the majority of the vacuum deposited film is consisted of elements with a low boiling point. However, the elements with a high boiling point (B, Ti, and Fe) have also been found in Figure 1,B. It suggests that these impurities may also exist as volatile compounds in MG-Si.

2. Vacuum Treatment in a Crystal Puller

In the past, we have used the phase separation technique repeatedly and with good reproducibility to remove the slag floating on top of the MG-Si melt. After the seed with the attached slag is removed from the melt, the seed is raised in the puller upper chamber and the isolation gate valve is closed. After cooling, the old seed is removed, a new seed is inserted and the upper chamber is purged for at least 1/2 hour before growth can be initiated.

To speed up this sequence we have considered two alternatives: One is the vacuum treatment of the melt, and the other is the concept of the double-walled crucible. The vacuum treatment was studied in this quarter. As indicated in Section II-1 vacuum evaporation may be a potential technique for removing some impurities from molten MG-Si. In the present experiment we have subjected MG-Si nuggets to reduced pressure both in the solid and molten state.

Following initial pumpdown to a vacuum of 0.5 torr the furnace was fired. There was immediately a vacuum deterioration probably due to interstitial H_2O outgassing. Outgassing did persist however as the temperature was increased well above the boiling point of H_2O, indicating that some volatile impurities were leaving the melt. The original vacuum was eventually restored in about an hour at a temperature close to the melting point of silicon. The increased pressure during heating corresponds to the evaporation of impurities as demonstrated in Section III-1. When all the silicon was melted

it started to boil vigorously almost immediately; at the same time the surface of the melt was getting progressively cleaner. In 5-10 minutes the slag had completely disappeared. At this time, since the furnace was not equipped for vacuum growth, the furnace had to be backfilled with Ar and a pull rod with the seed inserted into the chamber before regular growth could take place.

2.1 Results and Discussion

The experimental results indicate that the vigorous boiling of molten silicon can splash the floating impurities off the melt surface. Figure 2,A shows the slag floating on the silicon melt. Figure 2,B shows the melt boiling with some slag still left. Finally Figure 2,C shows a slag-free melt ready for an ingot growth. The impurity concentration at the seed and tang end of a vacuum-slagged MG-Si ingot is listed in Table IV. For comparison the impurity concentration of an ingot in which the slag was removed by physical means is also shown.

There seems to be a reduction by a factor of 3 for some transition metals and Al, with the notable exception of Fe. Although these results seem encouraging, the impurity concentration reduction obtained by vacuum-treating the silicon melt is not high enough, especially in the light of the close relationship between grain size and impurity concentration, to be of any significance. Nevertheless, the method seems to be a viable alternative to the removal of slag by physical means.

The effect of vacuum treatment of MG-Si melts will be studied further when the second Hamco puller, which has vacuum growth capability, becomes available. At that time, we will compare the impurity concentration of large-grained (almost single crystal) ingots grown under reduced pressure with ingots grown under Ar atmosphere, thus eliminating the grain boundary effect.

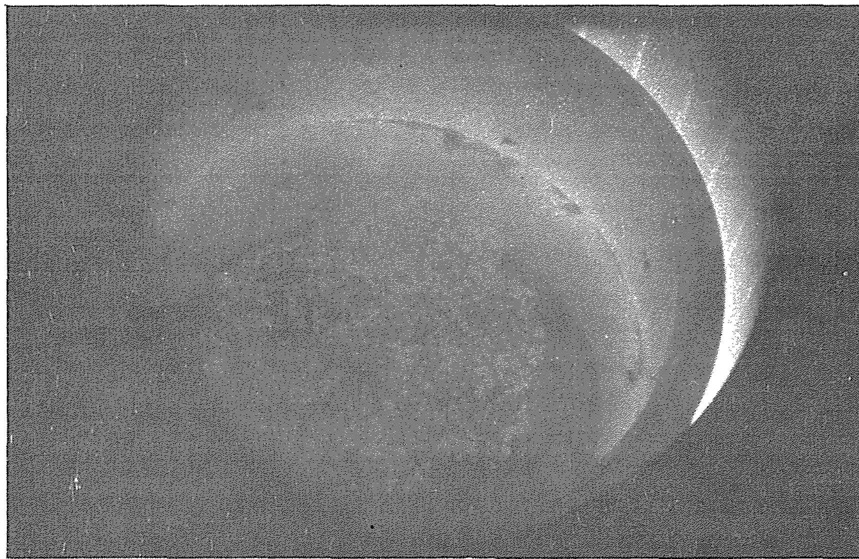

(A)

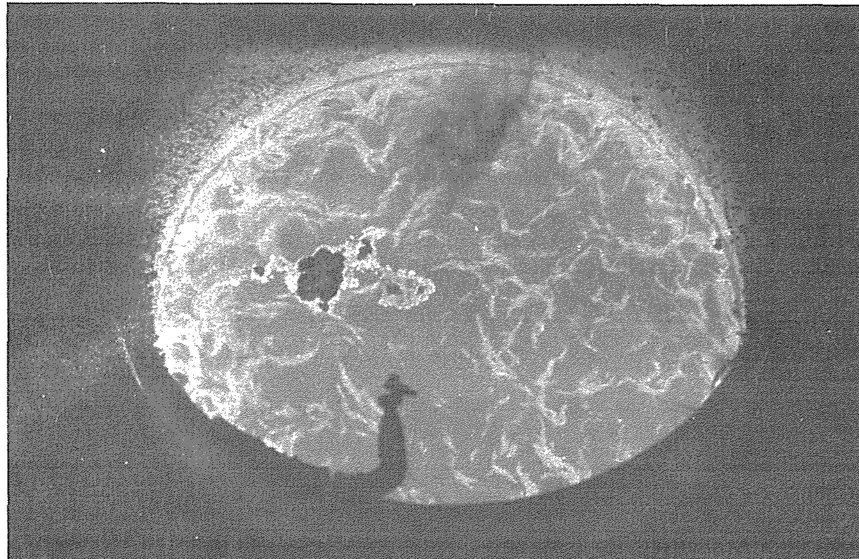

(B)

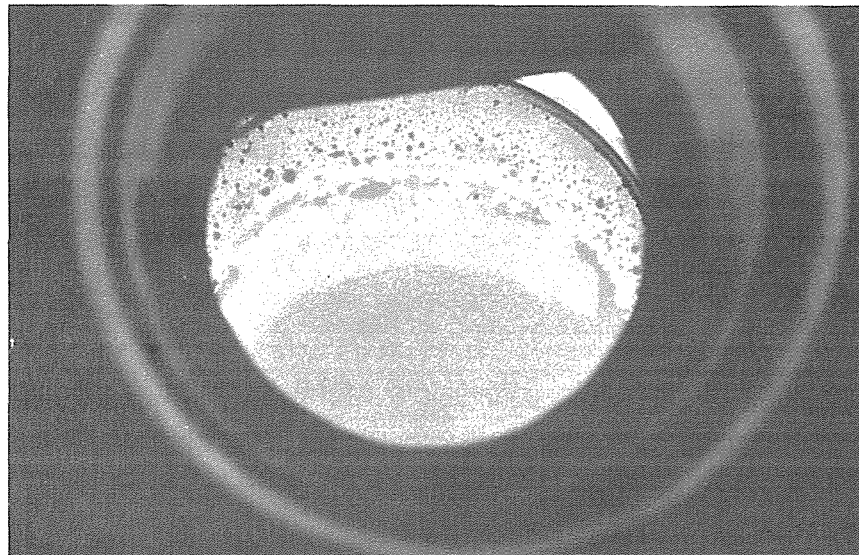

(C)

Figure 2. Disappearance of slag from MG-Si melt by vacuum treatment. (A) slag on MG-Si melt, (B) melt boiling, and (C) melt free of slag.

TABLE IV

COMPARISON OF IMPURITY CONCENTRATION IN MG-Si INGOTS PULLED FROM MELTS PURIFIED BY:

(A) VACUUM TREATMENT OF SLAG
(B) PHYSICAL SEPARATION OF SLAG

	(A) VACUUM TREATMENT PRIOR TO INGOT GROWTH		(B) SLAG REMOVAL BY PHYSICAL MEANS	
ELEMENT	MG-190(S)	MG-190(T)	MG-192(S)	MG-192(T)
Cr	10	100	100	330
Ca	1	33	10	100
Sr	<5	<5	<5	5
Mn	10	100	100	330
Al	100	330	330	1000
Fe	≥1000	>1000	>1000	>1000
Ni	≤5	10	10	33
Co	<5	5	5	10
Zr	<10	10	<10	33
Ti	10	100	33	100
Cu	≤1	33	10	33
Be	<1	<1	<1	<1
V	<5	<33	10	33
Mg	<1	<1	≤1	≤1
B	<10	<10	<10	<10
Sn	<5	<5	<5	<5

3. Purification by Impurity Redistribution

As outlined in Section II-2 impurity redistribution during ingot pulling is perhaps the most effective method of purifying MG-Si melts. Ingot growths were carried out in a Hamco 800 crystal puller. Quartz crucibles - 8" wide-were used to contain molten silicon. The melt size used in each experiment was 4 Kg. Slag was removed from molten silicon either by vacuum treament or by mechanical means. Ingot growth was always done in an argon ambient even in the cases in which slagging was done under vacuum. Three inch ingots were grown with pull rates varying from 1 to 3"/hour. Only first pulled ingots were considered in this study. Wafers were sliced from the seed and tang end of the ingots for evaluation.

In order to achieve large grain growth we have used a technique combining a large seed, to initiate growth, together with slow pull rate to delay the onset of constitutional supercooling. We have used a 3" shoulder for our experiments. Figure 3 shows a picture of such a shoulder. The shoulder was cut from a dislocation-free (100) crystal. No attempts were made to use a (111) shoulder as a seed. After growth the shoulder can be cut again and reused.

Careful blending of the large seed with the silicon melt is necessary if one wants to avoid the formation of voids in the growing ingot. Figure 4 shows three consecutive sections cut just below the seed in an ingot grown using a large seed. Void-induced polycrystalline growth is evident.

3.1 Results and Discussion

3.1.1 Impurity Concentration as Function of Distance from the Seed

Early experiments using a large shoulder as a seed had shown that the grain size was greatly increased only at the position 1 to 2 inches below the seed. However the grain size decreased dramatically

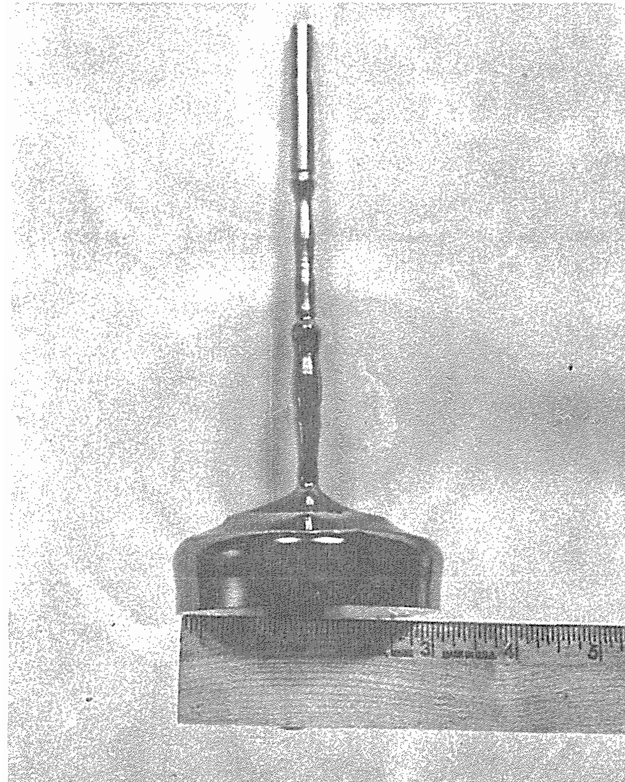

Figure 3. Three inches (100) shoulder used to initiate ingot growth.

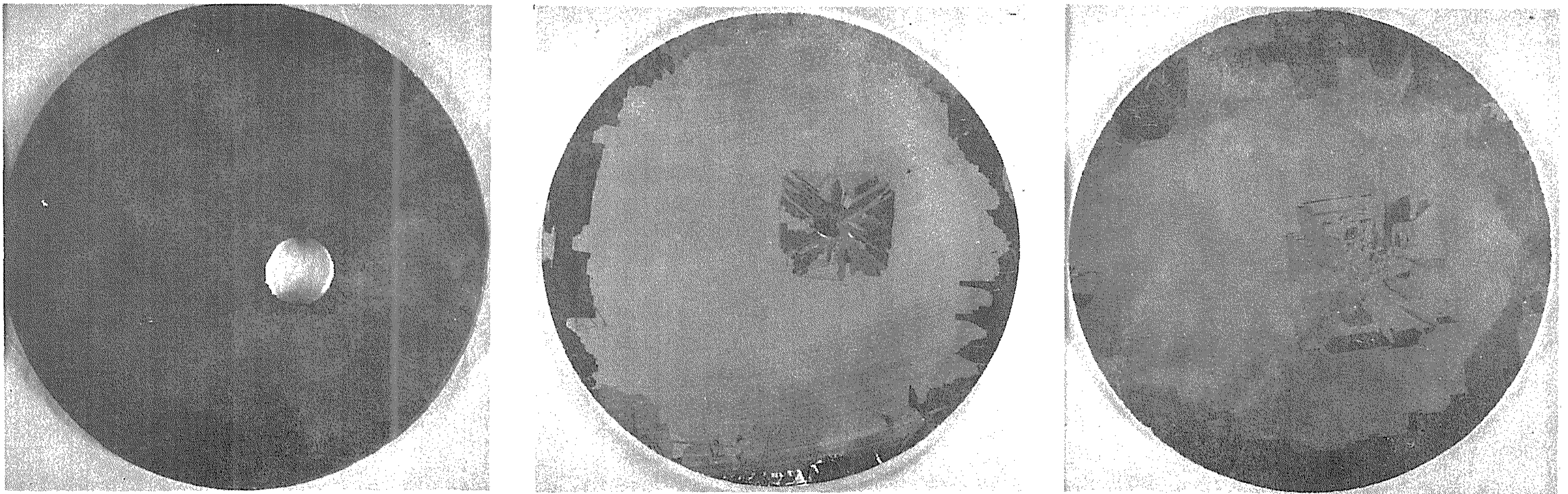

Figure 4. Polycrystalline growth induced by poor blending of a large seed with the silicon melt.

from there toward the tang end of the ingots. No difference in grain size was observed at the tang end compared to those grown from a smaller diameter seed. Figure 5 shows an 8 inch long crystal pulled at a rate of 3.5 inches/hour. Section 1, cut approximately 2 inches below the seed, still exhibits large grains bound by approximately perpendicular grain boundaries with the inner portion continuing the (100) seed orientation. Further cuts however show the grain structure considerably deteriorating as shown in sections 2, 3 and 4. The impurity concentration for the four sections and the seed and tang portion of the crystal is listed on Table V. The emission spectroscopy data indicate that there is an increase in impurities (especially metals) moving away from the seed (large grains) toward the tang end of the ingot (lamellar structure). A repeated experiment on another ingot showed a similar result.

3.1.2 Large Grains vs. Growth Rate

Figure 6,A shows 6 wafers cut from a MG-Si ingot grown at a rate of 3 inches/hour. The wafers were cut from a region extending about 1 inch below the seed. A progressive structure deterioration is evident. The effect of slowing the pull rate is manifested in Figure 6,B which shows 5 wafers cut from a MG-Si ingot grown at a rate of 1 inch/hour. The wafers were cut in the same portion of crystal below the seed as in the first ingot. There is no evidence of constitutional supercooling in Section 5 which is still almost completely single crystal.

Figure 7 compares grain size at the seed and tang ends of 3 MG-ingots. The ingot grown at 3"/hour with a small seed exhibits small polygonal grains at the seed end with a lamellar structure at the tang end

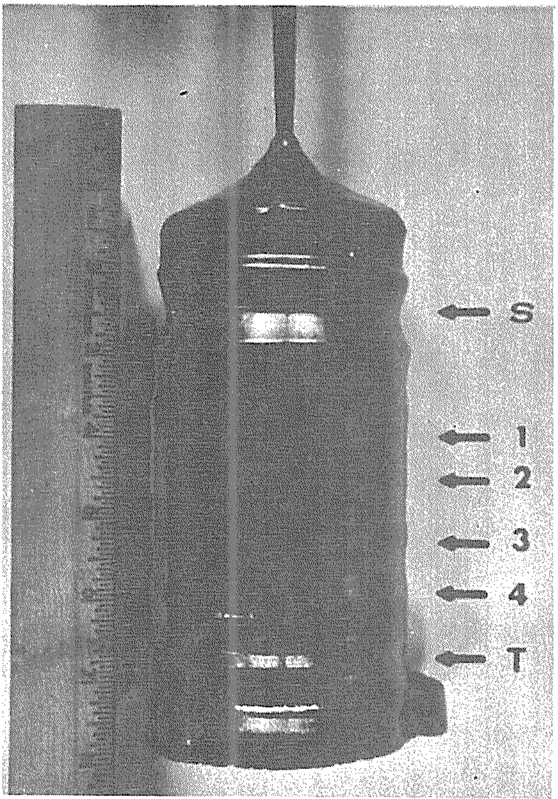

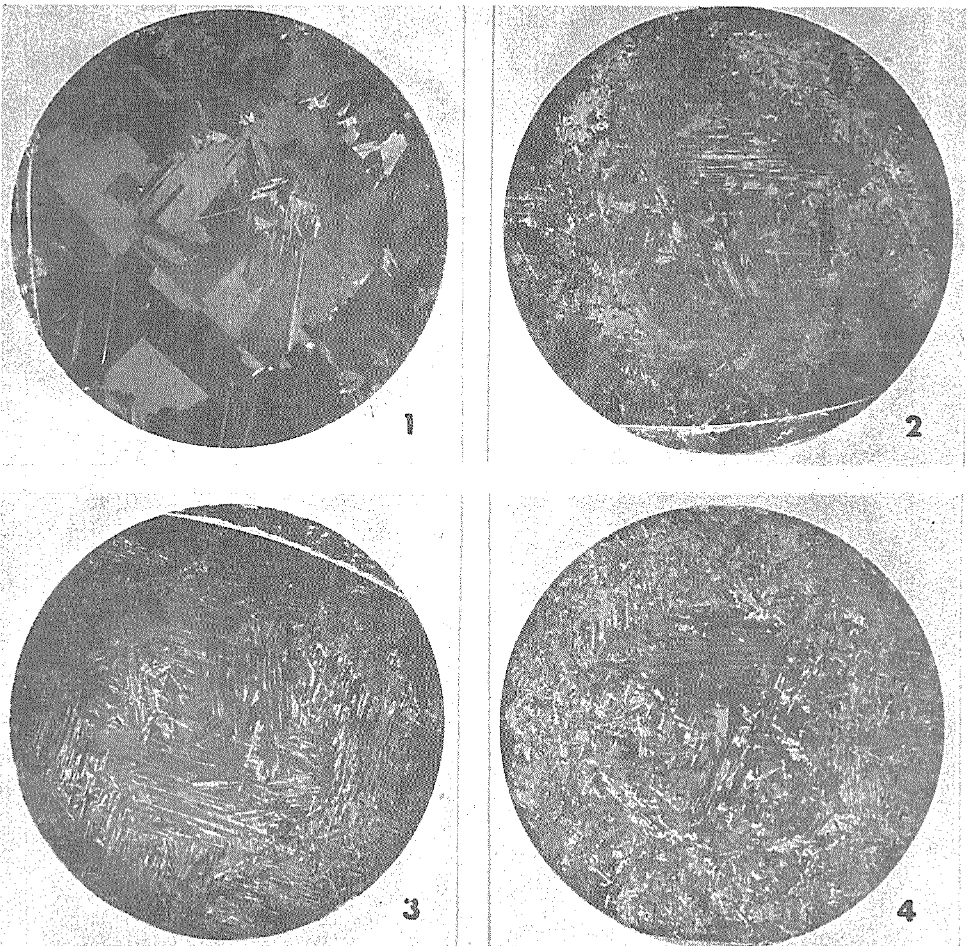

Figure 5. MG-Si ingot grown using a 3" (100) shoulder as a seed and relative cross sections.

TABLE V

VARIATION OF IMPURITY CONCENTRATION ALONG THE LENGTH OF A MG-SI INGOT.
ANALYSIS BY EMISSION SPECTROSCOPY (PPM W)

Element	MG-187(S)	MG-187(1)	MG-187(2)	MG-187(3)	MG-187(4)	MG-187(T)
Cr	<5	<5	10	10	10	33
Ce	<1	<1	<1	<1	<1	<1
Sr	<5	<5	<5	<5	<5	<5
Mn	<10	<10	33	33	33	100
Al	<5	<5	100	100	100	100
Fe	<2	<2	1000	1000	1000	1000
Ni	<5	<5	10	10	33	33
Co	<5	<5	5	5	5	5
Zr	<10	<10	<10	10	10	<10
Ti	<1	<1	100	100	100	100
Cu	<1	<1	<1	<1	<1	≤1
Be	<1	<1	<1	<1	<1	<1
V	<10	<10	33	100	100	100
Mg	<1	<1	33	33	33	10
B	<2	<2	<2	<2	<2	<2
Sn	<5	<5	<5	<5	<5	<5

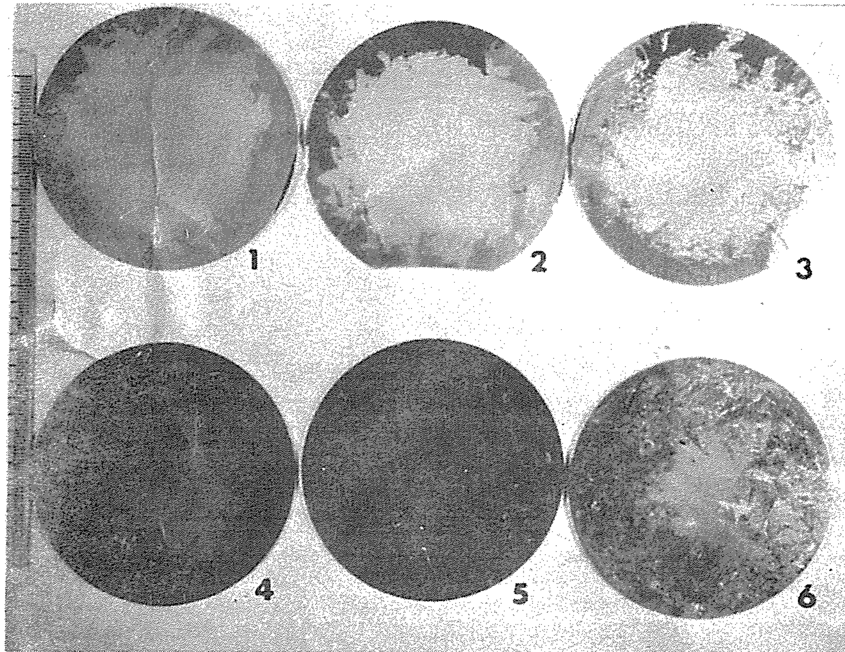

(A) Growth rate: 3 inches/hour

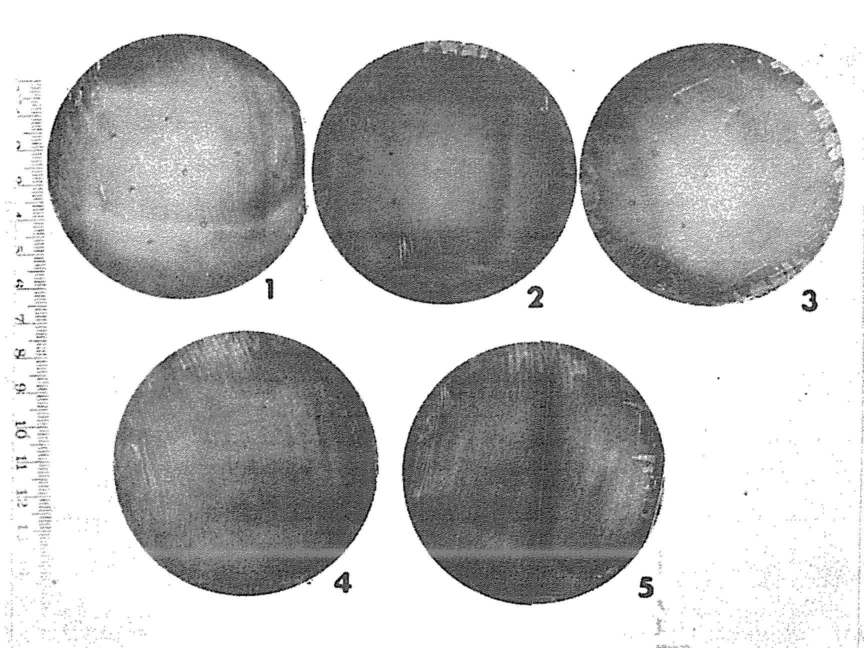

(B) Growth rate: 1 inch/hour

Figure 6. Comparison of grain size as a function of growth rate and distance from the seed.

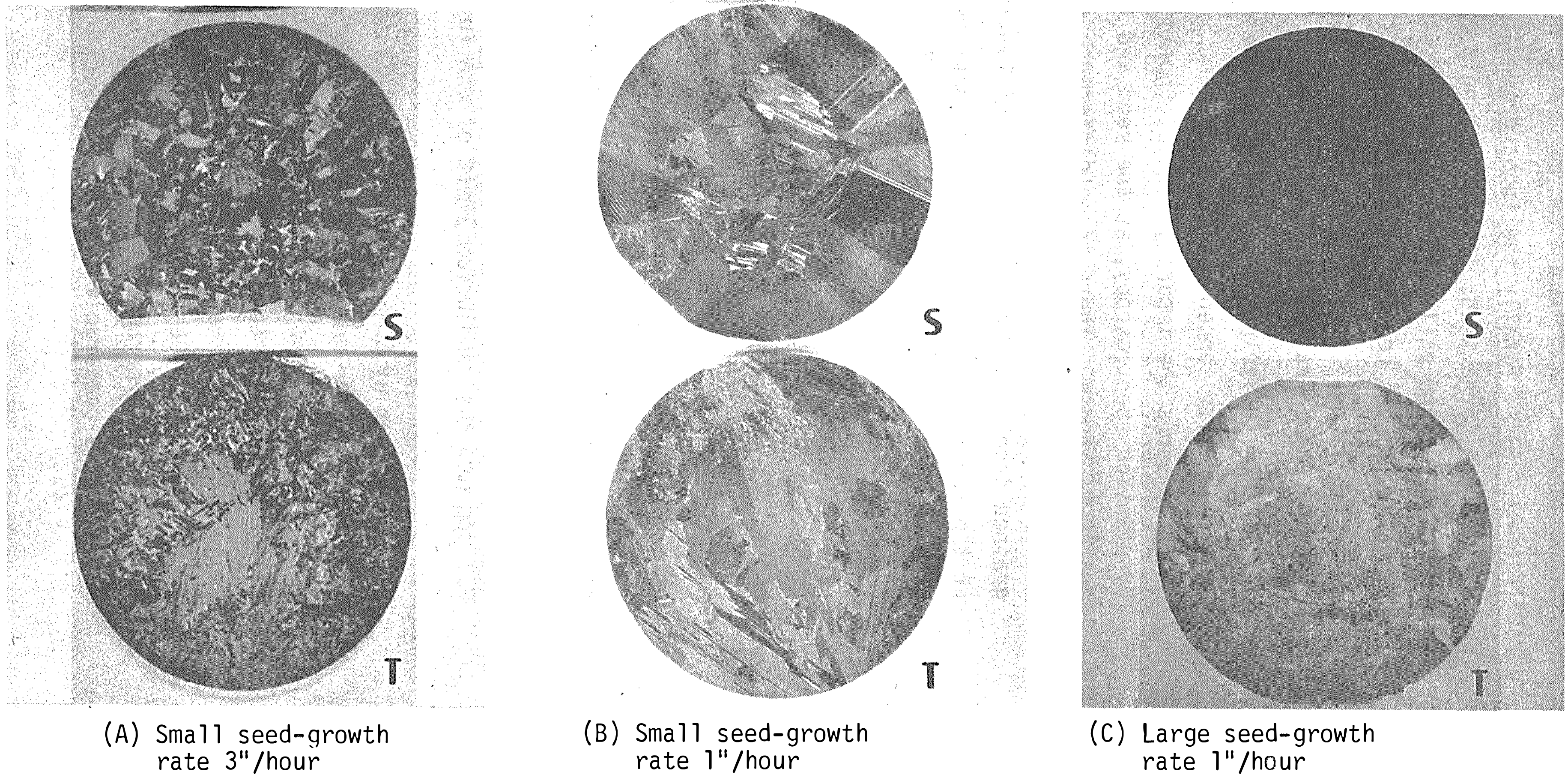

(A) Small seed-growth rate 3"/hour

(B) Small seed-growth rate 1"/hour

(C) Large seed-growth rate 1"/hour

Figure 7. Comparison of grain size as a function of seed size and growth rate at the seed and tang ends of three MG-Si ingots.

(Figure 7,B). Finally the ingot grown at 1"/hour, utilizing a large seed, is almost single crystal at the seed end and still has large grains with lamellar structure in the center at the tang end (Figure 7,C).

3.1.3 Impurity Concentration vs. Grain Size

The strong influence exercised by the grain size on the impurity concentration is evident in Table VI which compares the impurity content (ppmw) analyzed by emission spectroscopy, at the seed and tang end of two MG-Si ingots. There is no difference in impurity concentration at the seed and tang end of the large-grained ingot. On the other hand the lamellar section at the tang end of the other ingot contains significant higher impurity content, notably: Fe, Ti, Al, V, Cr and Mn.

Since Table VI shows that all the impurities in the large-grained ingot are below the resolution limit of the emission spectroscopy technique the same samples were also measured by spark source mass spectrography (SSMS). Table VII shows a complete list of the elements seen in MG-Si ingots by SSMS. The elements not listed in the table are either undetectable (O_2, N, Hg), are present as an instrument source (Ta, Co) or are below 0.1 ppm wt, the resolution limit of the instrument.

Comparison by SSMS between two MG-Si ingots and two semiconductor grade (SG) Si crystals is shown on Table VIII. The two SG crystals were P-type, boron doped with resistivity in the range of 0.01-0.07 ohm-cm. The MG ingots were also P-type with resistivity in the range of 0.06 to 0.1 ohm-cm. With the exception of Al, P, B and perhaps Ti the impurity content of the MG ingots is comparable to that of the SG crystals.

TABLE VI

COMPARISON OF IMPURITY CONCENTRATION, AS A FUNCTION OF GRAIN SIZE AT THE SEED END AND TANG ENDS OF TWO Mg-Si INGOTS. (PPM wt)

Element	Large Grains MG-185(S)	Lamellar MG-185(T)	Large Grains MG-196(S)	Large Grains MG-196(T)
Cr	<5	100	<5	<5
Ca	<1	3.3	<1	<1
Sr	<5	<5	<5	<5
Mn	<1	100	<1	<1
Al	<5	330	<5	<5
Fe	<2	>1000	<5	<5
Ni	<5	33	<5	<5
Co	<5	10	<5	<5
Zr	<10	10	<10	<10
Ti	<1	330	<1	<1
Cu	<1	3.3	<1	<1
Be	<1	<1	<1	<1
V	<5	100	<10	<10
Mg	<1	10	<1	<1
B	<10	<10	<10	<10
Sn	<5	<5	<5	<5

TABLE VII

COMPARISON OF IMPURITY CONCENTRATION, AS A FUNCTION OF GRAIN SIZE AT THE SEED AND TANG ENDS OF TWO MG-Si INGOTS. ANALYSIS BY S.S. MASS SPECTROGRAPHY. (PPM WT)

Element	Large Grains MG-185(S)	Lamellar MG185(T)	Large Grains MG-196(S)	Large Grains MG-196(T)	Element
W	<0.11	0.12	< 0.11	<0.11	W
Gd	<0.11	1.1	<0.11	<0.11	Gd
Cd	<0.15	0.44	0.34	<0.15	Cd
Mo	0.10	0.96	< 0.11	<0.11	Mo
Ge	0.10	0.48	0.72	0.72	Ge
Cu	0.02	0.50	0.02	0.03	Cu
Ni	0.45	19	0.65	0.53	Ni
Fe	0.13	840	0.14	0.30	Fe
Mn	0.04	370	0.07	0.19	Mn
Cr	--	57	--	--	Cr
V	--	91	--	--	V
Ti	0.08	210	0.03	0.32	Ti
Ca	--	9.8	--	0.37	Ca
Cl	2.3	1.6	0.24	0.27	Cl
S	3.0	--	0.12	0.20	S
P	3.7	3.7	1.4	1.8	P
Al	60	3300	60	47	Al
Mg	0.15	36	--	0.11	Mg
Na	0.20	≤0.55	--	0.27	Na
C	12	28	3.4	3.4	C
B	0.42	0.73	0.28	0.28	B

TABLE VIII

COMPARISON OF IMPURITY CONCENTRATION AT THE SEED AND TANG ENDS OF TWO LARGE GRAINED MG-Si INGOTS WITH SG CRYSTALS
ANALYSIS BY S.S. MASS SPECTROGRAPHY (PPMW)

Element	MG-195(S)	MG-195(T)	MG-196(S)	MG-196(T)	T36R07*	L-62**	Element
W	<0.11	<0.11	<0.11	<0.11	<0.11	<0.11	W
Gd	<0.11	<0.11	<0.11	<0.11	<0.11	<0.11	Gd
Cd	<0.15	<0.15	0.34	<0.15	<0.15	<0.15	Cd
Mo	0.12	0.13	<0.11	<0.11	<0.11	0.16	Mo
Ge	0.24	0.36	0.72	<0.72	--	--	Ge
Cu	0.02	0.02	0.02	0.03	0.01	0.01	Cu
Ni	<0.29	0.32	0.65	0.53	--	0.39	Ni
Fe	0.16	<0.09	0.14	0.30	0.10	0.10	Fe
Mn	<0.05	0.07	0.07	0.19	0.07	0.07	Mn
Ti	0.15	0.23	0.03	0.32	0.08	0.03	Ti
Ca	--	--	--	0.37	0.42	--	Ca
K	--	--	--	0.50	--	--	K
Cl	2.1	2.4	0.24	0.27	0.24	0.18	Cl
S	0.40	0.60	0.12	0.20	0.20	0.17	S
P	0.65	1.1	1.4	1.8	0.37	0.28	P
Al	82	39	60	47	0.16	0.07	Al
Mg	0.16	--	--	0.11	--	--	Mg
Na	--	--	--	0.27	0.10	--	Na
F	--	0.10	--	--	0.17	--	F
C	6.0	4.0	3.4	3.4	1.6	3.4	C
B	0.55	0.28	0.28	0.04	0.04	0.66	B

* 0.04 - 0.07 Ωcm, P-type (Boron)
** 0.01 - 0.03 Ωcm, P-type (Boron)

IV. CONCLUSIONS AND RECOMMENDATIONS

It has been shown in the previous paragraph that, with the exception of B, P, Al and Ti, the impurity content of first pulled MG-Si ingots can approach that of SG crystals. Phosphorus and boron are difficult to remove because of their unfavorable K. Fortunately, both impurities give shallow energy levels in the band gap and they are not expected to degrade solar cell performance. Recent data[5] indicate that about 6×10^{18} atoms cm^{-3} of phosphorus can be tolerated in P-type silicon, without adverse effect. This is well above the concentration of 8×10^{16} atoms cm^{-3} found in our MG-Si ingots by SSMS.

Aluminum and titanium on the other hand have been found to affect solar cell efficiency even at lower concentrations[5,6]. We feel that these are the two key elements that limit solar cell performance by lowering the lifetime of solar cells directly fabricated on MG-Si substrates without an epi layer. Consequently we will concentrate in reducing the Al and Ti content in MG-Si ingots to levels comparable to those found in SG silicon.

V. PLANS FOR THE NEXT QUARTER

In the next quarter we plan to perform:

(1) Optimize the purification steps

(2) Growth of large ingots (4-5" diameter) with large grain sizes

(3) Epitaxial deposition

(4) Solar cell fabrication and evaluation.

REFERENCES

1. Ming Liaw, Frank Secco d'Aragona, Bill Ingle and Don Down, Quarterly Technical Progress Report No. 1, DOE/SERI-8119-3/1, Feb. (1980).

2. Ming Liaw and Frank Secco d'Aragona, Quarterly Technical Progress Report No. 2, DOE/SERI-8119-3/2 May (1980).

3. S. E. Bradshaw and A. I. Mlavski, J. Electronics, 2 134 (1956).

4. M. Patel, Private communication.

5. R. H. Hopkins and Associates, "Silicon Materials Task of the Low Cost Solar Array Project," 15th Quarterly Report, April-June 1979.

6. A. Rohatgi, J. R. Davis, R. H. Hopkins, P. Rai-Choudbury, P. G. McMullin and J. R. McCormick, Solid State Electronics, 23, 415 (1980).